



OPEN

Relationship between right and left ventricle function in subjects free of cardiovascular diseases: a population-based MRI study

Ricarda von Krüchten¹, Roberto Lorbeer², Susanne Rospleszcz¹, Annette Peters^{3,4,5}, Stefan Karrasch^{4,6,7}, Holger Schulz^{5,7}, Bernard E. Bulwer⁸, Charlotte Wintergerst¹, Esther Askani¹, Thierno D. Diallo¹, Fabian Bamberg¹, Christopher L. Schlett¹ & Blerim Mujaj^{1,9}  

Right (RV) and left ventricular (LV) volumetric measurements by cardiac magnetic resonance imaging (MRI) are established for assessing systolic and diastolic function, but the role of MRI-derived lung volumes in LV function remains unclear. This study investigated the relationship between RV and LV function, considering lung volumes. In the KORA-MRI cohort, 361 subjects underwent 3 T whole-body MRI. Cardiac functional parameters were measured from cine-steady-state free precession sequences using cvi42. Lung volumes were derived semi-automatically with an in-house algorithm. Linear regression analyses assessed RV-LV relationships, adjusted for age, sex, cardiovascular risk factors, and lung volumes. Among 361 subjects (mean age 56.1 ± 9.1 years; 43% women), RV end-diastolic volume was positively associated with LV end-diastolic ($\beta = 28.1$, $p < 0.001$), end-systolic ($\beta = 11.0$, $p < 0.001$), and stroke volume ($\beta = 17.0$, $p < 0.001$), but inversely with ejection fraction ($\beta = -1.4$, $p = 0.001$). RV end-systole was positively associated with LV end-diastolic ($\beta = 21.2$, $p < 0.001$), end-systolic ($\beta = 11.5$, $p < 0.001$), stroke volume ($\beta = 9.7$, $p < 0.001$), and inversely with ejection fraction ($\beta = -3.3$, $p < 0.001$). Adjusting for lung volumes did not alter RV-LV associations, and no effect modification by sex was observed despite lung volume differences. In individuals without cardiovascular disease, RV and LV volumetric parameters were strongly associated, supporting the critical role of RV function in LV function, independent of lung volumes.

Keywords Cardiovascular imaging, Cardiac function, Lung volumes, Magnetic resonance imaging, Epidemiology

Abbreviations

BSA	Body surface area
cine-SSFP	Cine steady-state free precession
COPD	Chronic obstructive pulmonary disease
CT	Computed tomography
eGFR	Estimated glomerular filtration rate

¹Department of Diagnostic and Interventional Radiology, Medical Center, Faculty of Medicine, University of Freiburg, Hugstetter Straße 55, 79106 Freiburg, Germany. ²Department of Radiology, University Hospital of Munich, Ludwig-Maximilians-University, Marchioninistraße 15, 81377 Munich, Germany. ³Chair of Epidemiology, Institute for Medical Information Processing, Biometry and Epidemiology, Medical Faculty, Ludwig-Maximilians-University Munich, Marchioninistr. 15, 81377 Munich, Germany. ⁴Institute of Epidemiology, Helmholtz Zentrum München - German Research Center for Environmental Health, Ingolstädter Landstraße 1, 85764 Neuherberg, Germany. ⁵German Center for Diabetes Research (DZD), Partner Site Neuherberg, Ingolstädter Landstraße 1, 85764 Neuherberg, Germany. ⁶Institute and Outpatient Clinic for Occupational, Social and Environmental Medicine, University Hospital of Munich, Ludwig-Maximilians-University, Ziemssenstraße 1, 80336 Munich, Germany. ⁷Member of the German Center for Lung Research, Comprehensive Pneumology Center Munich (CPC-M), Max-Lebsche-Platz 31, 81377 München, Germany. ⁸Noninvasive Cardiology - Echocardiography Department, Cardiovascular Division, Brigham and Women's Hospital, Boston, MA, USA. ⁹General Practice, Huisartsenpraktijk, Bremstraat 116, 9320 Aalst, Belgium.  email: blerim.mujaj@gmail.com

FOV	Field of view
HOMA-IR	Homeostasis model assessment-insulin resistance index
IGT	Impaired glucose tolerance
IQRs	Interquartile ranges
KORA	Cooperative Health Research in the Region of Augsburg
LV	Left ventricle
LVEF	Left ventricle ejection fraction
MRI	Magnetic resonance imaging
OGTT	Oral glucose tolerance test
RV	Right ventricle
SD	Standard deviation
TE	Echo time
TR	Repetition time

Global cardiac function assessment relies on the measurement of diastolic and systolic function of the left ventricle (LV), with LV ejection fraction (LVEF) being the most widely used¹. The LVEF is a well-established parameter used for the diagnosis, clinical decision-making, and risk stratification of patients with cardiovascular diseases, with echocardiography^{2,3}, computed tomography (CT)⁴, and magnetic resonance imaging (MRI)⁵ being the primary diagnostic tools. The LVEF represents the volume of blood ejected into the systemic circulation during each contractile cycle, with right ventricle (RV) ejection fraction serving the pulmonary circulation, which includes the lungs and pulmonary vasculature. During diastole, RV and pulmonary pressures are directly exposed to LV filling pressures, and more broadly to global LV performance. The LV can maintain the systemic circulation even in the presence of RV dysfunction⁶. However, with diseases of the pulmonary vasculature and in the presence of impaired LV systolic or diastolic function, RV function becomes essential for maintaining cardiac output⁷. Therefore, right-heart function, which involves the RV, the pulmonary circulation, and lung function, including lung volumes, impacts LV function and vice versa. This becomes clinically evident in patients with cor pulmonale, heart failure with reduced LV ejection fraction (HFREF), and heart failure with preserved LV ejection fraction (HFpEF).

The relationships between LV and RV function, the pulmonary circulation, and lung parameters, including lung mass and volumes, as well as compensatory mechanisms involved with impaired cardiac function, are not well characterized⁸. Whether lung volumes directly impact or modify RV and LV function is unclear. Moreover, evidence of whether RV function influences LV function directly or through the pulmonary circulation remains sparse. From a community screening perspective, asymptomatic or at-risk patients with HFpEF, elevated LV filling pressures due to LV stiffness and impaired LV filling could be reflected in the pulmonary vasculature and lung function, thereby impacting lung volumes and RV function. Whole-body MRI has the advantage of simultaneous assessment of both lung volumes and volumetric LV and RV cardiac function within a single MRI scan⁹. To date, no study has simultaneously investigated these relationships.

Therefore, we aimed to investigate the relationship between lung volumes and global LV and RV function in subjects free of cardiovascular diseases within the population-based Cooperative Health Research in the Region of Augsburg (KORA)-MRI study.

Results

Table 1 summarizes the characteristics of the study population, with a mean age of 56.1 ± 9.1 years, and 43% of the subjects were women. Diabetes mellitus was prevalent in 12.5% of subjects. Median fasting glucose was 5.5 mmol/L, and median fasting insulin was 54.7 pmol/L. Hypertension was present in 33.2% of subjects, and 24.9% of subjects were on antihypertensive medication. Among the subjects, 20.8% were current smokers, the mean BMI was 28.0 ± 4.8 , and the mean BSA was 1.95 ± 0.22 . In all subjects, the mean lung volume was 3.98 ± 1.12 , and the prevalence of a history of COPD was 4.7%. The mean eGFR was 87.1 ± 13 . According to categories of lung volume tertiles, RV end-diastole, end-systole, and ejection fraction differed significantly between low, middle, and high tertiles. For LV, subjects in the high tertile of lung volumes had higher LV mass compared to middle and low tertile (Supplementary Table S1).

Association between RV and LV function parameters

We found significant associations between RV and LV functional parameters. RV end-diastolic volume was positively associated with LV end-diastolic volume, systolic volume, stroke volume, peak ejection rate, early diastolic rate, late diastolic rate, and mass, and inversely associated with ejection fraction (Table 2). RV end-systolic volume was positively associated with LV end-diastolic volume, systolic volume, stroke volume, peak ejection rate, early diastolic rate, and mass, and inversely associated with ejection fraction, but not with late diastolic rate (Table 2). RV stroke volume was positively associated with LV end-diastolic volume, systolic volume, stroke volume, ejection fraction, peak ejection rate, early diastolic rate, late diastolic rate, and mass (Table 2). RV ejection fraction was associated with LV stroke volume, ejection fraction, and late diastolic rate, and inversely associated with end-systolic volume, but not with end-diastolic volume, peak ejection rate, early diastolic rate, and mass (Table 2). The association between RV and LV did not attenuate after adjustment in all models, including model 2, and no effect modification was observed by lung volumes. In sensitivity analyses by excluding subjects with a history of COPD, the results were confirmatory (Supplementary Table S2).

Stratified analysis according to categories of lung volumes

In stratified analysis, according to lung volume tertiles (Fig. 1, Supplementary Tables S3 – S14), in subjects with higher lung volumes RV end-diastolic volume was positively associated with LV end-diastolic volume,

	All	Female	Male	P
N	361	154 (43%)	207 (57%)	
Age, years	56.1 (± 9.1)	56.1 (± 9.1)	56.1 (± 9.1)	0.977
Body mass index, kg/m ²	28.0 (± 4.8)	27.6 (± 5.5)	28.2 (± 4.2)	0.247
Body surface area, m ²	1.95 (± 0.22)	1.79 (± 0.17)	2.07 (± 0.17)	<0.001
Smoking status				0.136
Never, (%)	131 (36.3%)	63 (40.9%)	68 (32.9%)	
Past, (%)	155 (42.9%)	57 (37.0%)	98 (47.3%)	
Current, (%)	75 (20.8%)	34 (22.1%)	41 (19.8%)	
Alcohol use, (g/day)	18.3 (± 22.3)	8.8 (± 14.3)	25.3 (± 24.4)	<0.001
History of COPD	17 (4.7%)	7 (4.6%)	10 (4.8%)	0.899
Diabetes status				0.019
Normal (%)	222 (61.5%)	107 (69.5%)	115 (55.6%)	
Prediabetes (%)	94 (26%)	34 (22.1%)	60 (29%)	
Diabetes (%)	45 (12.5%)	13 (8.4%)	32 (15.5%)	
Fasting glucose, mmol/L	5.50 (5.11;6.05)	5.27 (4.94;5.88)	5.64 (5.27;6.16)	<0.001
Fasting insulin, pmol/L	54.7 (37.2;81.0)	49.3 (35.4;78.0)	60 (38.3;87.1)	0.010
HOMA-index	2.20 (1.41;3.51)	1.96 (1.29;3.33)	2.55 (1.52;3.66)	0.004
Hypertension, (%)	120 (33.2%)	43 (27.9%)	77 (37.2%)	0.064
Systolic blood pressure, mm/Hg	120.3 (± 16.8)	112.9 (± 14.5)	125.9 (± 16.3)	<0.001
Diastolic blood pressure, mm/Hg	75.2 (± 9.9)	72.0 (± 8.6)	77.6 (± 10.2)	<0.001
Antihypertensive medication, (%)	90 (24.9%)	41 (26.6%)	49 (23.7%)	0.521
Total cholesterol, mmol/L	5.61 (± 0.95)	5.63 (± 0.9)	5.59 (± 0.98)	0.646
HDL Cholesterol, mmol	1.61 (± 0.46)	1.82 (± 0.46)	1.45 (± 0.38)	<0.001
LDL Cholesterol, mmol	3.58 (± 0.86)	3.50 (± 0.83)	3.64 (± 0.88)	0.130
Triglycerides, mmol	1.21 (0.87;1.75)	1.08 (0.77;1.37)	1.38 (0.97;2.12)	<0.001
Lipid lowering medication, %	39 (10.8%)	18 (11.7%)	21 (10.1%)	0.640
eGFR, ml/min/1.73 m ²	87.1 (± 13)	85.7 (± 13.3)	88.1 (± 12.7)	0.093
Lung Volumes, L	3.98 (± 1.12)	3.31 (± 0.71)	4.48 (± 1.10)	<0.001
cardiac parameters				
RV End-diastolic Volume, (mL)	165.6 (± 39.6)	144.2 (± 30.9)	181.4 (± 38.0)	<0.001
RV End-systolic Volume, (mL)	79.5 (± 25.8)	64.5 (± 18.9)	90.7 (± 24.6)	<0.001
RV Stroke Volume, (mL)	86.1 (± 19.5)	79.9 (± 17.1)	90.8 (± 20.0)	<0.001
RV Ejection fraction, (%)	52.6 (± 7.1)	55.7 (± 6.2)	50.3 (± 6.8)	<0.001
LV End-diastolic Volume, (mL)	130.6 (± 32.5)	118.2 (± 26.1)	139.8 (± 33.8)	<0.001
LV End-systolic Volume, (mL)	41.2 (± 18.1)	34.8 (± 14.7)	46.0 (± 19.0)	<0.001
LV Stroke Volume, (mL)	89.4 (± 20.1)	83.4 (± 16.9)	93.9 (± 21.2)	<0.001
LV Ejection fraction, (%)	69.2 (± 7.8)	71.1 (± 6.7)	67.8 (± 8.3)	<0.001
LV Peak ejection rate, (mL/s)	357.8 (± 133.6)	334.1 (± 107.3)	375.5 (± 148)	0.003
LV Early diastolic filling rate, (mL/s)	230.4 (± 115.5)	231.5 (± 106.4)	229.6 (± 122.1)	0.875
LV Late diastolic filling rate, (mL/s)	240.6 (± 141)	236.3 (± 134)	243.9 (± 146.2)	0.614
LV Mass, diastolic, g	141 (± 34.6)	114.5 (± 23.9)	160.6 (± 27.5)	<0.001

Table 1. Study population characteristics. The values represent mean \pm standard deviation (SD), median (interquartile ranges) or frequency along with percentage (%). P = p-value for difference (t-test, Mann-Whitney-U test or chi²-test); Abbreviation: eGFR = estimated glomerular filtration rate, HDL = high-density lipoprotein, HOMA-index = homeostasis model assessment -index, LDL = low-density lipoprotein; LV = left ventricle; RV = right ventricle.

end-systolic volume, stroke volume, peak ejection rate, early diastolic rate, but not with ejection fraction, late diastolic rate and ventricle mass. Similarly, RV end-systolic volume was associated with LV end-diastolic volume, end-systolic volume, stroke volume, peak ejection rate, early diastolic rate, and ventricle mass, inversely with ejection fraction, but not with late diastolic rate, similarly to middle and high tertiles. RV stroke volume was associated with LV end-diastolic volume, end-systolic volume, stroke volume, peak ejection rate, early diastolic rate, late diastolic rate, and ventricle mass, but not with ejection fraction, similarly to middle and high tertiles. RV ejection fraction was associated with LV stroke volume, ejection fraction, late diastolic rate, and inversely with end-systolic volume but not with end-diastolic volume, peak ejection rate, early diastolic rate, and mass, while in the middle tertile and high tertile, the association with late diastolic rate became non-significant.

PER SD	Model 1	P	Model 2	P	Model 3	P	Model 4	P
LV EDV								
RV EDV	28.1 (26.0; 30.1)	<0.001	27.9 (25.8; 29.9)	<0.001	27.2 (25.1; 29.4)	<0.001	26.8 (24.6; 29.1)	<0.001
RV ESV	21.2 (18.3; 24.0)	<0.001	21.0 (18.2; 23.9)	<0.001	19.6 (16.7; 22.5)	<0.001	18.9 (16.0; 21.8)	<0.001
RV SV	25.1 (23.1; 27.1)	<0.001	25.0 (23.0; 27.0)	<0.001	24.5 (22.4; 26.7)	<0.001	24.1 (21.9; 26.3)	<0.001
RV EF	0.3 (-3.0; 3.6)	0.855	0.06 (-3.2; 3.3)	0.969	-0.2 (-3.4; 2.9)	0.87	0.1 (-3.0; 3.3)	0.922
LV ESV								
RV EDV	11.0 (9.3; 12.7)	<0.001	10.9 (9.2; 12.7)	<0.001	11.1 (9.3; 12.9)	<0.001	10.8 (9.0; 12.6)	<0.001
RV ESV	11.5 (9.8; 13.2)	<0.001	11.4 (9.7; 13.1)	<0.001	11.2 (9.4; 12.9)	<0.001	10.8 (9.1; 12.6)	<0.001
RV SV	6.3 (4.6; 8.1)	<0.001	6.2 (4.4; 8.0)	<0.001	6.1 (4.2; 8.0)	<0.001	5.8 (3.9; 7.7)	<0.001
RV EF	-5.5 (-7.3; -3.7)	<0.001	-5.6 (-7.4; -3.8)	<0.001	-5.6 (-7.4; -3.8)	<0.001	-5.3 (-7.1; -3.5)	<0.001
LV SV								
RV EDV	17.0 (15.6; 18.4)	<0.001	16.9 (15.5; 18.3)	<0.001	16.1 (14.6; 17.6)	<0.001	16.0 (14.5; 17.5)	<0.001
RV ESV	9.7 (7.6; 11.7)	<0.001	9.6 (7.5; 11.6)	<0.001	8.4 (6.4; 10.4)	<0.001	8.0 (6.0; 10.1)	<0.001
RV SV	18.7 (18.0; 19.5)	<0.001	18.7 (17.9; 19.4)	<0.001	18.4 (17.5; 19.2)	<0.001	18.2 (17.4; 19.1)	<0.001
RV EF	5.8 (3.7; 7.8)	<0.001	5.6 (3.6; 7.7)	<0.001	5.3 (3.3; 7.2)	<0.001	5.4 (3.5; 7.3)	<0.001
LV EF								
RV EDV	-1.4 (-2.3; -0.5)	0.001	-1.4 (-2.3; -0.5)	0.002	-1.6 (-2.6; -0.7)	0.001	-1.5 (-2.5; -0.5)	0.002
RV ESV	-3.3 (-4.1; -2.4)	<0.001	-3.3 (-4.1; -2.4)	<0.001	-3.4 (-4.3; -2.5)	<0.001	-3.3 (-4.2; -2.4)	<0.001
RV SV	1.1 (0.2; 1.9)	0.01	1.1 (0.2; 1.9)	0.009	1.1 (0.2; 2.0)	0.011	1.2 (0.3; 2.1)	0.006
RV EF	4.0 (3.2; 4.7)	<0.001	4.0 (3.3; 4.8)	<0.001	3.9 (3.2; 4.7)	<0.001	3.8 (3.1; 4.6)	<0.001
LV PEAK EJECTION RATE								
RV EDV	102 (90; 114)	<0.001	102 (91; 114)	<0.001	101 (89; 113)	<0.001	101 (89; 113)	<0.001
RV ESV	71.7 (57.6; 85.8)	<0.001	71.5 (57.4; 85.6)	<0.001	66.1 (52.0; 80.2)	<0.001	65.2 (50.9; 79.6)	<0.001
RV SV	98.0 (87.6; 108)	<0.001	98.6 (88.1; 109)	<0.001	99.7 (89.0; 110)	<0.001	98.7 (87.7; 109)	<0.001
RV EF	14.3 (-0.3; 28.9)	0.055	14.0 (-0.6; 28.6)	0.061	13.5 (-0.5; 27.7)	0.06	13.6 (-0.6; 27.9)	0.061
LV EARLY DIASTOLIC RATE								
RV EDV	84.3 (74.3; 94.2)	<0.001	83.7 (73.8; 93.7)	<0.001	83.4 (73.3; 93.4)	<0.001	84.0 (73.7; 94.4)	<0.001
RV ESV	58.8 (46.9; 70.7)	<0.001	58.3 (46.4; 70.2)	<0.001	53.5 (41.7; 65.3)	<0.001	53.3 (41.2; 65.4)	<0.001
RV SV	80.8 (71.9; 89.6)	<0.001	80.4 (71.5; 89.3)	<0.001	82.7 (73.9; 91.6)	<0.001	82.5 (73.4; 91.6)	<0.001
RV EF	11.4 (-0.8; 23.7)	0.068	10.7 (-1.5; 22.9)	0.086	11.8 (0.1; 23.5)	0.048	11.7 (-0.1; 23.6)	0.054
LV LATE DIASTOLIC RATE								
RV EDV	37.8 (21.5; 54.0)	<0.001	36.5 (20.2; 52.7)	<0.001	34.3 (17.0; 51.6)	<0.001	29.3 (11.9; 46.7)	0.001
RV ESV	9.4 (-7.4; 26.2)	0.271	8.7 (-8.0; 25.4)	0.309	3.6 (-13.6; 20.9)	0.68	0.1 (-17.1; 17.4)	0.986
RV SV	54.8 (40.5; 69.1)	<0.001	53.6 (39.2; 68.0)	<0.001	55.9 (40.6; 71.3)	<0.001	50.8 (35.3; 66.3)	<0.001
RV EF	33.2 (18.1; 48.4)	<0.001	32.4 (17.3; 47.5)	<0.001	34.0 (18.8; 49.2)	<0.001	32.3 (17.2; 47.5)	<0.001
LV MASS								
RV EDV	8.8 (5.8; 11.8)	<0.001	8.9 (5.9; 11.9)	<0.001	9.0 (6.2; 11.7)	<0.001	8.5 (5.7; 11.3)	<0.001
RV ESV	5.3 (2.2; 8.4)	0.001	5.4 (2.2; 8.5)	0.001	5.7 (2.9; 8.5)	<0.001	5.0 (2.1; 7.8)	0.001
RV SV	9.3 (6.6; 12.0)	<0.001	9.5 (6.7; 12.2)	<0.001	9.0 (6.4; 11.5)	<0.001	8.9 (6.3; 11.4)	<0.001
RV EF	2.2 (-0.6; 5.1)	0.131	2.2 (-0.6; 5.1)	0.125	1.1 (-1.4; 3.7)	0.392	1.7 (-0.8; 4.3)	0.189

Table 2. Association between right ventricle function parameters and left ventricle function parameters. The beta estimate given with a 95% confidence interval represents the estimate size between RV and LV function from linear regression model. The model 1 = adjusted for sex and age; model 2 = model 1 + lung volumes; model 3 = model 2 + smoking, alcohol use, BMI, systolic blood pressure, diastolic blood pressure, diabetes mellitus, total cholesterol and eGFR; model 4 = model 3 + insulin, glucose, antihypertensive medication, lipid lowering medication; CI = 95% confidence interval; SD = standard deviation. Abbreviation: BMI = body mass index; EDV = end-diastolic volume; EF = ejection fraction; eGFR = estimated glomerular filtration rate, ESV = end-systolic volume; LV = left ventricle, RV = right ventricle; SV = stroke volume.

Stratified analysis according to sex

In females (Fig. 2, Supplementary Tables S15 – S18), RV end-diastolic volume was associated with LV end-diastolic volume, end-systolic volume, stroke volume, peak ejection rate, early diastolic rate, late diastolic rate, and ventricle mass, but not with ejection fraction. RV end-systolic volume was associated with LV end-diastolic volume, end-systolic volume, stroke volume, peak ejection rate, early diastolic rate, and ventricle mass, inversely with ejection fraction, but not with late diastolic rate. RV stroke volume was associated with LV end-diastolic volume, end-systolic volume, stroke volume, peak ejection rate, early diastolic rate, late diastolic rate, and ventricle mass, but not with ejection fraction. RV ejection fraction was associated with LV stroke volume,

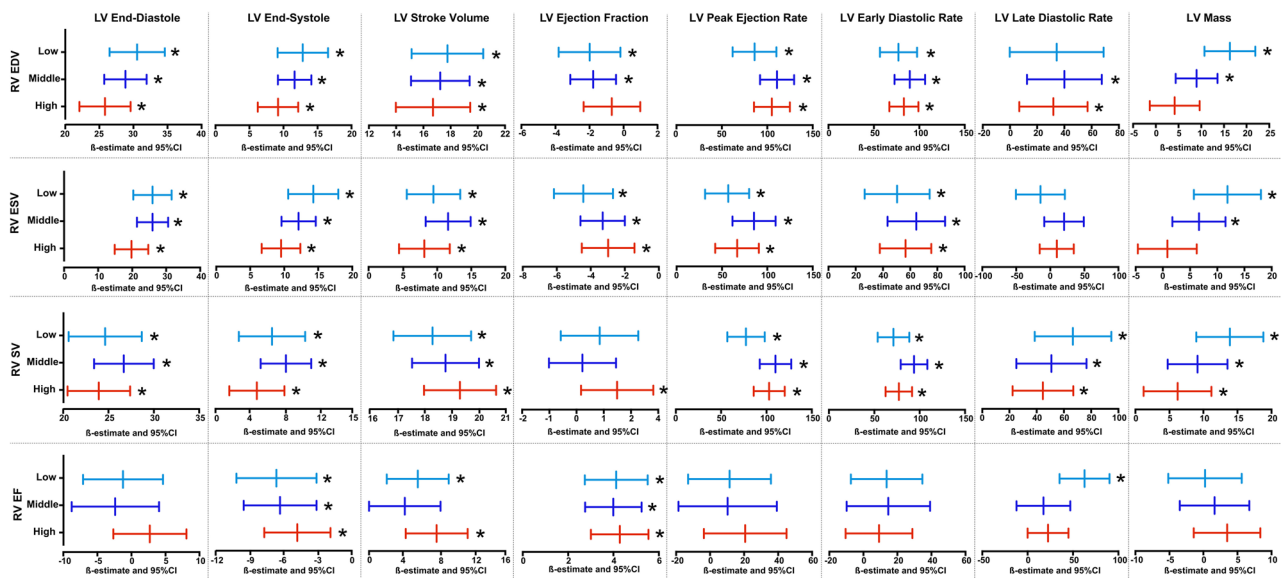


Fig. 1. Flowchart of the study. Abbreviations: BMI = body mass index; BP = blood pressure; BSA = body surface area; CAD = cardiovascular disease; COPD = chronic obstructive pulmonary disease; DBP = diastolic blood pressure; DM = diabetes mellitus; eGFR = estimated glomerular filtration rate; HOMA-IR = homeostasis model assessment-insulin resistance index; IGT = impaired glucose tolerance; LV = left ventricle; OGTT = oral glucose tolerance test; PAD = peripheral artery disease; RV = right ventricle; SBP = systolic blood pressure.

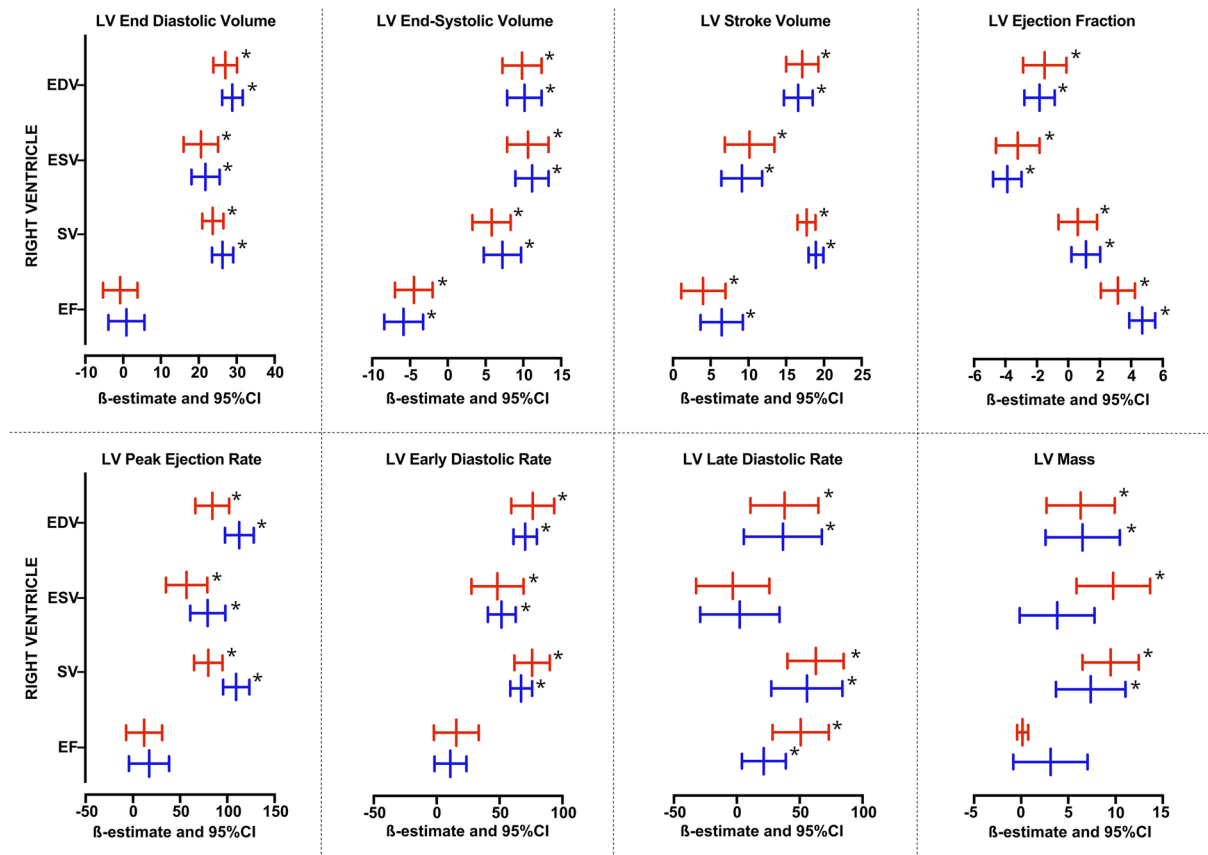


Fig. 2. The relationship between right ventricle function parameters and left ventricle function parameters, according to tertiles of lung volumes (light blue—low, blue—middle, and red—high). The β -estimate with 95% confidence interval depicts the effect size for each parameter from linear regression model adjusted for age and sex. Asterisks denotes p -value < 0.05 .

ejection fraction, late diastolic rate, and inversely with end-systolic volume but not with end-diastolic volume, peak ejection rate, early diastolic rate, and mass. In males (Fig. 2, Supplementary Tables S19 – S22), RV end-diastolic volume was associated with LV end-diastolic volume, end-systolic volume, stroke volume, peak ejection rate, early diastolic rate, late diastolic rate, ventricle mass, and inversely with ejection fraction. RV end-systolic volume was associated with LV end-diastolic volume, end-systolic volume, stroke volume, peak ejection rate, early diastolic rate, and ventricle mass, inversely with ejection fraction, but not with late diastolic rate. RV stroke volume was associated with LV end-diastolic volume, end-systolic volume, stroke volume, ejection fraction, peak ejection rate, early diastolic rate, late diastolic rate, and ventricle mass. RV ejection fraction was associated with LV stroke volume, ejection fraction, late diastolic rate, and inversely with end-systolic volume but not with end-diastolic volume, peak ejection rate, early diastolic rate, and mass.

Methods

Study population

Subjects from the region of Augsburg, Germany, aged between 25 and 74 years, were recruited in the KORA-MRI study¹⁰. Participants were examined at the KORA study center between June 2013 and September 2014, and a 3 Tesla whole-body MRI scan was performed¹⁰. Inclusion criteria for undergoing a whole-body MRI scan included prediabetes, diabetes for the control group, and written informed consent for all participants. Exclusion criteria were age > 74 years, participants with a known history of coronary artery disease, myocardial infarction, stroke, peripheral artery disease, pregnancy, unavailable oral glucose test, poor overall health condition, or other physical limitations. In addition, subjects with contraindications to MRI scan, such as known gadolinium contrast allergy, cardiac stents, cardiac pacemaker or implantable defibrillator, implanted metal parts, breast-feeding women, subjects with claustrophobia, and subjects with impaired renal function were excluded. From a total of participants with an MRI scan (n = 400), subjects with incomplete MRI data and/or inadequate image quality were excluded. Hence, 361 subjects were included in the analysis (Fig. 3).

The KORA-MRI study was compiled according to the Helsinki Declaration on Human Research¹¹ and approved by the Institutional Research Ethics Board of the Medical Faculty of Ludwig-Maximilian University, Munich.

Whole-body MR imaging protocol

A 3-Tesla MRI system (MagnetomSkyra, Siemens AG, Healthcare Sector, Erlangen, Germany)¹⁰ was applied to perform the whole-body MRI scans using an 18-channel body surface coil and a table-mounted spine matrix coil. The protocol included sequences covering the entire body from the head to the femur, including particular organs, e.g., brain, carotid arteries, tissue/organ quantification, and fat compartments. A 2-point DIXON T1 sequence was used to analyze the lung in submaximal inspiration breath-hold and an acquisition time of 15 s. Slice thickness was 3 mm, coronal acquisition, including a field of view (FOV) of 488 mm x 716 mm, a matrix of 256 x 256, a repetition time (TR) of 4.06 ms, and an echo time (TE) of 1.26 ms. For analysis of the heart, the cine-steady-state free precession sequence was acquired in a short-axis view with 10 layers and 25 phases. Slice thickness was 8 mm, including a FOV of 297 mm x 360 mm, a matrix of 240 x 160, a TR of 29.97 ms, a TE of 1.46 ms, and a flip angle of 62°.

MR-Image analysis for cardiac measurements

Cine steady-state free precession (cine-SSFP) sequences were used to imaging cardiac function, morphology, and morphology diseases. LV and RV function were evaluated using commercially available Cvi42 software (version 4.1.5(190)); Circle Cardiovascular Imaging Inc. (Calgary, Alberta, Canada). Detection of LV contours and calculation of LV volumes was processed automatically, and if necessary, corrected manually according to guidelines¹², and LV myocardial mass was assessed during end-diastole. After manually segmenting the lumen of the RV in the end-systole and end-diastole in each layer from the cardiac apex to the pulmonary valve¹³, the software automatically calculated the corresponding volumes. The difference between the end-systolic and end-diastolic volumes comprises the stroke volume and ejection fraction parameters. Furthermore, filling and ejection rates for LV were quantified using pyHeart, a dedicated in-house software displaying LV time-volume-curves^{14,15}. Peak gradients were assessed during systolic ejection and early LV filling, an active process involving LV diastolic suction and recoil, and late LV filling caused by atrial contraction¹⁶.

MR Image analysis for lung volume

An algorithm was used to automatically process the MR images for quantification of lung volumes, as described previously^{9,17}. The algorithm was trained to perform the following segmentation steps: Correction of intensity inhomogeneities, pre-extraction of a coarse region of interest containing the airways, segmentation of bilateral lungs and trachea region, extraction of the trachea, separating the lung into right and left lung, and refining the lung region. Pulmonary blood vessels outside the mediastinal contours were included in the lung region⁹. An independent reader visually checked the MRI scans set after the automated processing, unaware of the clinical information, and high-quality outputs of the algorithm framework have been verified⁹.

Covariates

Information on risk factors was obtained through physical examination, interview, and blood sampling. Body mass index (BMI) and body surface area (BSA) were calculated based on height and weight, smoking status, history of chronic obstructive pulmonary disease (COPD), alcohol use (g/day), and antihypertensive medication were assessed by questionnaire. According to the WHO criteria, diabetes state was defined as prediabetes (impaired glucose tolerance, IGT: normal fasting glucose concentration and a 2-h serum oral glucose tolerance test (OGTT) glucose concentration between 140 and 200 mg/dL; and/or an impaired fasting glucose

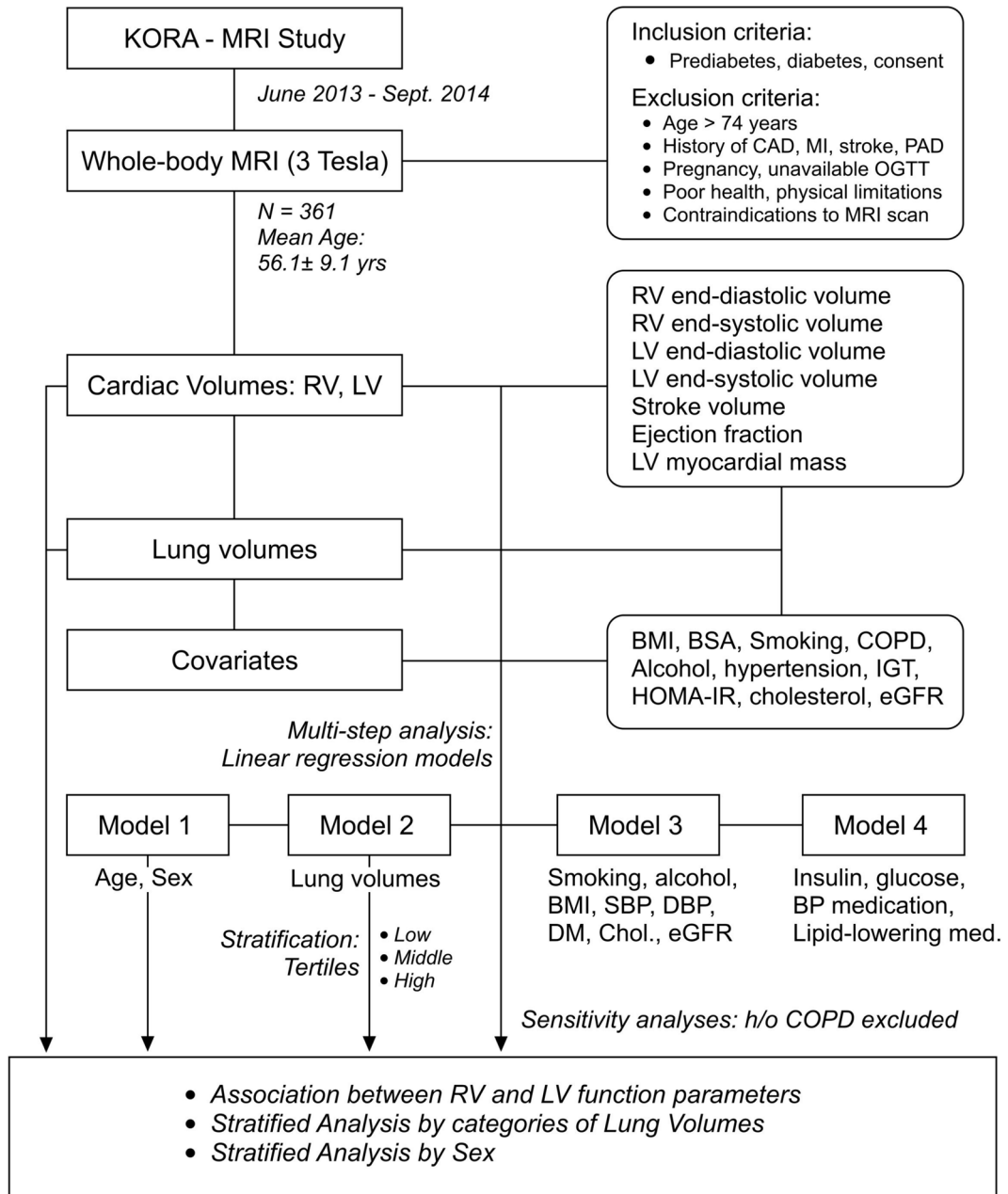


Fig. 3. The relationship between right ventricle function parameters and left ventricle function parameters, according to sex (red-female, blue-male). The univariate β -estimate with 95% confidence interval depicts the effect size for each parameter from linear regression model adjusted for age. Asterisks denotes p -value < 0.05 .

concentration, as defined by fasting glucose levels between 110 and 125 mg/dL, and a normal 2-h serum glucose concentration), and diabetes (2-h serum glucose concentration as determined by OGTT that was > 200 mg/dL and/or a fasting glucose level that was > 125 mg/dL¹⁸.

The homeostasis model assessment-insulin resistance index (HOMA-IR) was calculated using the formula: [fasting glucose (mmol/L) x fasting insulin (μ U/L)/22.5]¹⁹. Hypertension was defined as systolic blood pressure > 140 mmHg, diastolic blood pressure > 90 mmHg, or receiving current antihypertensive treatment. Using an enzymatic colorimetric method (Dimension Vista 1500, Siemens Healthcare Diagnostics, Eschborn, Germany, or Cobas c702, Roche Diagnostics GmbH, Mannheim, Germany) the total serum cholesterol and serum creatinine concentrations were analyzed. The estimated glomerular filtration rate (eGFR) was calculated based on creatinine/cystatin C or combination according to a standardized formula²⁰.

Statistical analysis

The distribution of population characteristics was described by using mean and standard deviation (SD), median (interquartile ranges (IQRs)), or percentages for continuous and categorical variables, respectively. We used a

multi-step approach analysis, first using linear regression models, we investigated the association between RV and LV functional parameters. In Model 1, we adjusted for sex and age. Model 2 was adjusted for lung volumes, and Model 3 additionally for smoking, alcohol use, BMI, systolic blood pressure, diastolic blood pressure, diabetes mellitus, total cholesterol, and eGFR. Model 4 was additionally adjusted for insulin, glucose, antihypertensive, lipid-lowering medication. Second, by stratifying the subjects per lung volumes (tertiles) categories in low, middle, and high, using the above-mentioned linear regression models, we assessed the association between RV and LV function parameters. Third, stratified analyses for sex were performed using the same models in linear regression analysis. In sensitivity analyses, subjects with a history of COPD were excluded, and the same models in linear regression analysis were performed. A p-value of < 0.05 was considered statistically significant. All analyses were performed using Stata (Stata 16.1 Corporation, College Station, TX, USA).

Discussion

In subjects free of cardiovascular diseases, RV function was associated with LV function independently of lung volumes. Furthermore, lung volumes did not modify the relationship between RV and LV. Despite dissimilar hemodynamics, especially the marked differential between right- and left-sided intracardiac pressures, these findings confirm strong coupling between the RV and LV. Therefore, although the lungs are a constituent part of pulmonary circulation, LV function parameters remain closely coupled with the RV's.

Previously, our group investigated the relationship between RV and LV with lung volumes, with evidence that LV stroke volume and LV early diastolic filling rate were inversely associated with lung volumes¹⁵. This suggests that lung volumes may be an effect modifier or confounder of LV function. Given the previous observations on the possible association between lung volumes with RV and LV¹⁵, we tested the hypothesis of effect modification.

Normal LV diastolic filling is an active process (LV diastolic suction) involving active diastolic recoil and relaxation at normal filling pressures. Although this is intimately reflected in the pulmonary circulation and RV function, the degree to which pulmonary function, specifically lung volumes, impacts RV and LV remains unclear. To date, our study is the first study to simultaneously assess the relationship of cardiac volumes along with lungs as volumetric tissue mass. In the previous population-based MESA study, the effect of pulmonary vasculature on pulmonary function and dyspnea was investigated. This study reported that lower pulmonary vascular volume was associated with lower LV end-diastolic volume, stroke volume, and cardiac output among subjects with a long-term smoking history²¹. Similarly, within the MESA study, the role of a greater extent of emphysema was assessed, and this study reported that airflow obstruction was linearly related to impaired LV filling and overall lower cardiac output²². The study sheds light on structural respiratory changes in advanced respiratory diseases where the lungs can directly trigger compensatory mechanisms to increase the lung mass and compensate for oxygenation capacity. However, there was no evidence on RV functional capacity from emphysema patients undergoing surgery, although a recent study showed that the effect of lung volume reduction improved LV filling and cardiac performance²³. In this context, our findings provide additional evidence combining information from three key organs: the RV, the lung, and the LV.

Whole-body MRI, and its capacity to simultaneously assess both pulmonary and global cardiac function, could potentially deliver distinct advantages for assessing patients at risk for developing²⁴. Cardiometabolic risk factors (e.g., hypertension, diabetes, dyslipidemia, and smoking) and increasing age are major risk factors for HFrEF, and such patients often pose a diagnostic and therapeutic challenge as they present with pulmonary symptoms (dyspnea and exertional fatigue), but with normal LV volumes and ejection fraction. Hence, the simultaneous assessment of both pulmonary and cardiac parameters using whole-body MRI is potentially promising in this population.

Given the fact that the vast majority of participants were free of active respiratory disease (95.3%), lung volume differences were observed, and all participants had preserved cardiac volumes. The relationship between RV and LV was examined by adjusting lung volumes in an attempt to explore the modification mechanisms of lung volumes on the relationship between RV and LV. Observations revealed that, despite the potential modification by lung volumes, RV and LV function parameters remain coupled. However, our results should not be interpreted in the context of pulmonary blood flow or pulmonary microvascular measurements²¹.

The complex relationship between cardiac volumetric parameters and lung volumes may be explained by various risk factors affecting cardiac function, such as smoking^{21,25} and environmental factors²⁶, or by the influence of risk factors such as hypertension²⁷ and diabetes mellitus²⁸. Previously, we investigated the role of serum insulin on lung volume and observed that increased serum insulin levels were associated with decreased lung volume and RV function¹⁶. This confirms that the negative influence of various factors affects heart and lung function independently, and compensatory changes may not affect their mutual function²⁹.

The strengths of the study include the use of advanced 3 T whole-body MRI technology with a detailed protocol that included a cine-steady-state free precession sequence for imaging of the heart and lungs among healthy individuals free of cardiovascular disease from a population-based cohort. In addition, whole-body MRI allows simultaneous assessment of the heart and lungs within a single time point for reliable real-time cardio-pulmonary function evaluation. Further, automatic algorithms were used for MR image analysis of lung volumes and heart function volumes quantification. Furthermore, multivariable adjustment, stratified analysis, and sensitivity analysis by excluding COPD patients were applied to confirm the results. However, our study encounters limitations that need to be addressed. First, although the MRI protocol for cardiac imaging included atria, atrial function was not used in the adjustment. Second, we used non-invasive imaging and could not assess blood flow within the pulmonary vascular system. Third, our findings generate hypotheses and require further confirmation in other designs and populations. Fourth, our study may represent a small sample that recruited a cohort of participants with European ancestry, and the generalizability may be limited to other geographic regions.

Conclusion

In subjects free of cardiovascular diseases, RV and LV parameters were strongly associated, suggesting that RV function is crucial for LV function. Given the critical role of the RV in the pulmonary circulation including lung volumes, lung volumes did not modify LV function in subjects without cardiovascular diseases.

Data availability

The datasets used and/or analyzed during the current study are available from the corresponding author on reasonable request. Alternatively, for access to KORA study data, requests can be directed to kora.passt@helmholtz-muenchen.de and are subject to approval by the KORA Board.

Received: 21 January 2025; Accepted: 25 November 2025

Published online: 29 January 2026

References

1. Cikes, M. & Solomon, S. D. Beyond ejection fraction: an integrative approach for assessment of cardiac structure and function in heart failure. *Eur. Heart J.* **37**, 1642–1650 (2016).
2. Haddad, F., Hunt, S. A., Rosenthal, D. N. & Murphy, D. J. Right ventricular function in cardiovascular disease, part I: Anatomy, physiology, aging, and functional assessment of the right ventricle. *Circulation* **117**, 1436–1448 (2008).
3. Nagueh, S. F. et al. Recommendations for the evaluation of left ventricular diastolic function by echocardiography: an update from the american society of echocardiography and the european association of cardiovascular imaging. *J. Am. Soc. Echocardiogr.* **29**, 277–314 (2016).
4. Yamamoto, M. et al. Cardiac functional analysis with multi-detector row CT and segmental reconstruction algorithm: comparison with echocardiography, SPECT, and MR imaging. *Radiology* **234**, 381–390 (2005).
5. Kramer, C. M. et al. Standardized cardiovascular magnetic resonance imaging (CMR) protocols: 2020 update. *J. Cardiovasc Magn Reson.* **22**, 17 (2020).
6. Haddad, F., Doyle, R., Murphy, D. J. & Hunt, S. A. Right ventricular function in cardiovascular disease, part II: pathophysiology, clinical importance, and management of right ventricular failure. *Circulation* **117**, 1717–1731 (2008).
7. Testani, J. M. et al. Effect of right ventricular function and venous congestion on cardiorenal interactions during the treatment of decompensated heart failure. *Am. J. Cardiol.* **105**, 511–516 (2010).
8. Lumens, J., Blanchard, D. G., Arts, T., Mahmud, E. & Delhaas, T. Left ventricular underfilling and not septal bulging dominates abnormal left ventricular filling hemodynamics in chronic thromboembolic pulmonary hypertension. *Am. J. Physiol. Heart Circ. Physiol.* **299**, H1083–H1091 (2010).
9. Mueller, J. et al. Automated MR-based lung volume segmentation in population-based whole-body MR imaging: correlation with clinical characteristics, pulmonary function testing and obstructive lung disease. *Eur Radiol.* **29**, 1595–1606 (2019).
10. Bamberg, F. et al. Subclinical disease burden as assessed by whole-body mri in subjects with prediabetes, subjects with diabetes, and normal control subjects from the general population: the KORA-MRI study. *Diabetes* **66**, 158–169 (2017).
11. World Medical Association Declaration of Helsinki: ethical principles for medical research involving human subjects. *Jama.* **310**, 2191–2194 (2013).
12. Grover, S., Leong, D. P. & Selvanayagam, J. B. Evaluation of left ventricular function using cardiac magnetic resonance imaging. *J. Nucl. Cardiol.* **18**, 351–365 (2011).
13. Schulz-Menger, J. et al. Standardized image interpretation and post processing in cardiovascular magnetic resonance: society for cardiovascular magnetic resonance (SCMR) board of trustees task force on standardized post processing. *J. Cardiovasc. Magn. Reson.* **22**, 19 (2013).
14. von Krüchten, R. et al. Serum insulin is associated with right ventricle function parameters and lung volumes in subjects free of cardiovascular disease. *Eur. J. Endocrinol.* **184**, 289–298 (2021).
15. von Krüchten, R. et al. Subclinical cardiac impairment relates to traditional pulmonary function test parameters and lung volume as derived from whole-body MRI in a population-based cohort study. *Sci. Rep.* **11**, 16123 (2021).
16. Caudron, J., Fares, J., Bauer, F. & Dacher, J. N. Evaluation of left ventricular diastolic function with cardiac MR imaging. *Radiographics* **31**, 239–259 (2011).
17. Ivanovska, T. et al. A fast and accurate automatic lung segmentation and volumetry method for MR data used in epidemiological studies. *Comput. Med. Imaging Graph.* **36**, 281–293 (2012).
18. Definition and diagnosis of diabetes mellitus and intermediate hyperglycemia: report of a WHO/IDF consultation. *World Health Organization.* (2006).
19. Matthews, D. R. et al. Homeostasis model assessment: insulin resistance and beta-cell function from fasting plasma glucose and insulin concentrations in man. *Diabetologia* **28**, 412–419 (1985).
20. Levey, A. S. et al. A new equation to estimate glomerular filtration rate. *Ann. Intern. Med.* **150**, 604–612 (2009).
21. Aaron, C. P. et al. Pulmonary vascular volume, impaired left ventricular filling and dyspnea: the MESA lung study. *PLoS ONE* **12**, e0176180 (2017).
22. Barr, R. G. et al. Percent emphysema, airflow obstruction, and impaired left ventricular filling. *N. Engl. J. Med.* **362**, 217–227 (2010).
23. Jörgensen, K. et al. Effects of lung volume reduction surgery on left ventricular diastolic filling and dimensions in patients with severe emphysema. *Chest* **124**, 1863–1870 (2003).
24. Gevaert, A. B. et al. Heart failure with preserved ejection fraction: recent concepts in diagnosis, mechanisms and management. *Heart* **108**, 1342–1350 (2022).
25. Holmen, T. L., Barrett-Connor, E., Clausen, J., Holmen, J. & Bjermer, L. Physical exercise, sports, and lung function in smoking versus nonsmoking adolescents. *Eur. Respir. J.* **19**, 8–15 (2002).
26. Adam, M. et al. Adult lung function and long-term air pollution exposure. ESCAPE: a multicentre cohort study and meta-analysis. *Eur. Respir. J.* **45**, 38–50 (2015).
27. Schnabel, E. et al. High blood pressure, antihypertensive medication and lung function in a general adult population. *Respir. Res.* **12**, 50 (2011).
28. Litonjua, A. A., Lazarus, R., Sparrow, D., Demolles, D. & Weiss, S. T. Lung function in type 2 diabetes: the normative aging study. *Respir. Med.* **99**, 1583–1590 (2005).
29. Kotton, D. N. & Morrisey, E. E. Lung regeneration: mechanisms, applications and emerging stem cell populations. *Nat. Med.* **20**, 822–832 (2014).

Acknowledgements

The KORA study was initiated and financed by the Helmholtz Zentrum München – German Research Center for Environmental Health, which is funded by the German Federal Ministry of Education and Research (BMBF)

and by the State of Bavaria.

Author contributions

Study concept and design were performed by RVK and BM. Acquisition, analysis, or interpretation of data was performed by RVK, RL, FB, CLS, and BM. Drafting of the manuscript was performed by RVK and BM. Critical revision of the manuscript for important intellectual content was performed by RVK, RL, SR, AP, SK, HS, BEB, CW, EA, TD, FB, CLS, and BM. Statistical analysis was performed by RL. Administrative, technical, or material support was performed by RVK and BM. Study supervision: BM. All authors read and approved the final manuscript. RL had full access to all the data in the study and takes responsibility for its integrity and the data analysis.

Funding

Open Access funding enabled and organized by Projekt DEAL. The KORA study was initiated and financed by the Helmholtz Zentrum München—German Research Center for Environmental Health, which is funded by the German Federal Ministry of Education and Research (BMBF) and by the State of Bavaria. The study was funded by the German Research Foundation (DFG, Bonn, Germany; Project ID 245222810 and 519189125), the German Centre for Diabetes Research (DZD, Neuherberg Germany), and the German Centre for Cardiovascular Disease Research (DZHK, Berlin, Germany).

Declaration

Competing interests

The authors declare no competing interests.

Ethics approval

The study was performed in accordance with the Declaration of Helsinki, including written informed consent of all participants. All study methods were approved by the ethics committee of the Bavarian Chamber of Physicians, Munich, Germany (EC No. 06068). MRI examination protocol was further approved by the ethics committee of the Ludwig-Maximilians University Hospital, Munich, Germany. Informed consent as well as consent for publication was obtained from all participants involved in the study.

Additional information

Supplementary Information The online version contains supplementary material available at <https://doi.org/10.1038/s41598-025-30588-z>.

Correspondence and requests for materials should be addressed to B.M.

Reprints and permissions information is available at www.nature.com/reprints.

Publisher's note Springer Nature remains neutral with regard to jurisdictional claims in published maps and institutional affiliations.

Open Access This article is licensed under a Creative Commons Attribution 4.0 International License, which permits use, sharing, adaptation, distribution and reproduction in any medium or format, as long as you give appropriate credit to the original author(s) and the source, provide a link to the Creative Commons licence, and indicate if changes were made. The images or other third party material in this article are included in the article's Creative Commons licence, unless indicated otherwise in a credit line to the material. If material is not included in the article's Creative Commons licence and your intended use is not permitted by statutory regulation or exceeds the permitted use, you will need to obtain permission directly from the copyright holder. To view a copy of this licence, visit <http://creativecommons.org/licenses/by/4.0/>.

© The Author(s) 2026